Electronic Supplementary Material (ESI) for Journal of Materials Chemistry C.

Electronic Supplementary Information†

Small Molecule Doped Organic Crystals towards Long-Persistent Luminescence in Water and Air

Desissa Yadeta Muleta,[‡a] Jiawei Song,[‡a] Wenhui Feng,[‡b] Ruitao Wu,[c] Xueqin Zhou,[b] Wei Li,[b] Lichang Wang,[bc] Dongzhi Liu,[b] Tianyang Wang[*a] and Wenping Hu[*ad]

Table of contents

1. Experimental Section and Characterization data

Preparation of MDPA:DDF2o crystals. The trace-doped (1 mol%) MDPA:DDF2o powder (0.50 g) was dissolved in absolute ethanol (5 mL) at room temperature. Then, 50 mL of deionized water was added slowly into the solution with stirring in air. After sitting at room temperature for 6 h, the precipitate was filtered out of the suspension and collected as a white crystalline solid (0.48 g, 96.0%). The white MDPA crystals were prepared similarly to the MDPA:DDF2o crystals, the only difference being that MDPA powder was used in place of 1 mol% MDPA:DDF2o powder.

Preparation of the paint. MDPA:DDF2o crystals (0.50 g) with polyvinyl pyrrolidone (PVP) (0.60 g) were combined with deionized water (5 mL), then stirred at room temperature for 6 h to produce the milky-white paint.

Measurement and Characterization. A Rigaku Thermo plus TGA 2 instrument was used to perform thermogravimetric analysis (TGA), and a TA DSC Q 20 instrument was used for differential scanning calorimetry (DSC). Electrochemical properties were measured using cyclic voltammetry (CV) on a BAS 100W electrochemical analyzer. Ultraviolet photoelectron spectroscopy (UPS) was carried out using a Thermo Scientific ESCALab 250Xi. A Leica DM2700M optical microscope with the fluorescence plug-in unit was utilized for optical and fluorescence microscope images. Polarized microscope and SEM images were captured with a Nikon Eclipse Ci-POL polarized optical microscope and Hitachi JSM-7800F field emission microscope with an EDX spectrometer, respectively. Single-crystal X-ray diffraction was performed using a SuperNova diffractometer, which had a CCD detector and rotating-anode X-ray generator. Ultraviolet-visible (UV-vis) absorption was carried out with a NicoIet Evolution 300 UV evisible spectrometer, fluorescence spectra were obtained using a Varian CARY ECLIPSE fluorospectrophotometer, and transient photoluminescence spectra with a Edinburgh FLS1000 photoluminescence spectrometer. An Edinburgh FLS980 spectrophotometer was used to generate MDPA and DDF2o phosphorescence spectra at 77 K.

An Ocean optical fiber spectrophotometer was used to record spectra for photoluminescence, phosphorescence, and LPL of the MDPA crystals at room temperature. Time-correlated single photon counting (TC-SPC) was used to collect fluorescence decay emission spectra via picosecond diode lasers (Horiba Jobin Yvon Instruments). The Electronic Supplementary Information encompasses some details of TGA, DSC, CV, UPS, computation, and single-crystal X-ray diffraction analysis. [CCDC 2040167 (MDPA crystal) and 2040239 (MDPA:DDF2o crystal) contains the supplementary crystallographic data for this paper. These data can be obtained free of charge from The Cambridge Crystallographic Data Centre via www.ccdc.cam.ac.uk/data_request/cif.]

TGA. The thermal stability of the samples was determined by measuring the weight loss while heating at a rate of 10 ºC min^{-1} from 30 ºC to 700 ºC under inert nitrogen atmosphere.

DSC. The samples of MDPA and DDF2o were heated at a rate of 10 ºC min^{-1} from 30 ºC to 350 ºC under inert nitrogen atmosphere.

CV. The electrochemical properties were measured using a BAS 100W electrochemical analyzer utilizing the three-electrode configuration with a glassy carbon electrode as the working electrode, $Ag/AgNO_3$ electrode as the reference electrode, and platinum as the auxiliary electrode. The analyzer was calibrated using a ferrocene/ferrocenium redox couple as the external standard prior to the measurements. The scan rate was set to 30 mV/s. Dichloromethane containing 0.1 mol•L^{-1} tetra-butylammoniumhexafluorophosphate ($TBAPF_6$) was employed as the medium for the cyclic voltammetric determination. The compound concentration was 5×10^{-3} mol•L^{-1}.

UPS. The ultraviolet photoelectron spectroscopy (UPS) samples were prepared by spin-coating the solutions on quartz substrates. Samples were analyzed on Thermo Scientific ESCALab 250Xi using UPS, The gas discharge lamp was used for UPS, with helium gas admitted and the HeI (21.22eV) emission line employed. The helium pressure in the analysis chamber during analysis was about 3×10^{-8} mbar. The data were acquired with –10 V bias. The HOMO energy levels were calculated from $E_{\mathrm{HOMO}} = E_{\mathrm{cutoff}} - E_{\mathrm{onset}} - h\nu$, where E_{cutoff} and E_{onset} are obtained from the UPS spectra, hν is 21.22 eV.

Computations. Geometry optimizations of the molecules were carried out using the three-parameter exchange functional of Becke and correlation functional of Lee, Yang and Parr (B3LYP)[1-3] and the Perdew–Burke–Ernzerhof (PBE) functional[4] with the 6-311G(d,p) basis set in toluene without any symmetry constraints. The polarized continuum model (PCM) framework[5] was used to describe the solvent effect. The SCF convergence was 10^{-8} a.u. while the gradient and energy convergence was 10^{-4} a.u. and 10^{-5}a.u., respectively. All the calculations were performed using *Gaussian16* package.[6] In order to confirm the optimized geometry as a global minimum, frequency calculations at the same level of theory were performed. The calculations were performed following the same procedures as our previous work.[7-8] Calculations were also performed using VASP[9-10] to study single molecules and the crystal MDPA. The effective core potentials were described by the projector augmented wave (PAW) potentials[11-12] with a cutoff energy of 400 eV. The PBE functional was used to describe the exchange-correlation interactions. These calculations were performed following the same procedures as our previous work.[13-14] For single molecules, qualitative aggrements wereobtained between the calculations.

Single-crystal X-ray diffraction analysis. Single crystals of MDPA and MDPA:DDF2o were mounted on a loop, and data were collected with a SuperNova diffractometer with CCD detector equipped with a rotating-anode X-ray generator that emits graphite-monochromated Cu Kα radiation (λ=1.54184 Å). The empirical absorption correction using equivalent reflections and Lorentzian polarization was performed with the program Crystal Clear 1.3.6. The structures were solved with the program SHELXS-97 and refined against F^2 using

SHELXL-97.[15-16] Pertinent crystallographic data of the MDPA and MDPA:DDF2o single-crystals were exhibited in Table S2 of Supporting Information.

TC-SPC. Excitation of the samples were done with picosecond diode lasers (Horiba Jobin Yvon Instruments) at 321 nm or 375 nm, and the time resolution was ~ 150 ps. The laser pulse energy was ca. 15 pJ and attenuated (often by more than an order of magnitude) to the desired count rate of ca. 1% or less of the excitation frequency. A cooled (ca. -40°C) Hamamatsu MCP- photomultiplier R3809U 51 was used for detection of single photons, and the signal passed through a discriminator (Ortec 9307) and into a TAC (Ortec 566, 100 ns range used). The electrical trigger signal from the laser was also passed through a discriminator (Tennelec TC454) and on to the TAC (Ortec 566). The TAC output was read by a DAQ-1 MCA computer card using 1024 channels and collected with Horiba Jobin Yvon Data Station 2.5. Measurements were made in reverse mode at 5 MHz and under magic angle polarization. A cut-off filter, GG400 (Excitation at 321 nm) or GG 515 (Excitation at 375 nm), was used to block stray excitation light. A dilute solution of Ludox was used to record the instrument response function without any filter for solution measurements. No monochromator was used, i.e. all wavelengths transmitted by the cut-off filter were collected.

2. Supplementary table, figures and discussions

Table S1 Frontier orbital energies (HOMO and LUMO) and some energy level data upon excitation for DDF2o and MDPA. The energy of the CS state DDF2o$^{\bullet+}$-(MDPA)$_n$-MDPA$^{\bullet-}$ (E_{cs}, $n \geq 0$), estimated by the offset of the electrochemically measured HOMO and LUMO energies ($E_{cs} = -(E_{HOMO}^{DDF}-E_{LUMO}^{MDPA})$), was consistent with that of the 450 nm delayed fluorescence (2.8 eV)

sample	HOMO[a)]/eV	LUMO[b)]/eV	λ_{max}(abs)/nm	λ_{max}(fl)/nm	E(S$_1$)[c)]/eV	λ_{max}(ph)/nm	E(T$_1$)[(d)]/eV
DDF2o	-5.1	-2.1	382	400	3.2	515	2.4
MDPA	-5.7	-2.3	276	356	3.9	520	2.4

a) The HOMO energy was deduced from the oxidation onset potential and calculated by the equation: $E_{HOMO} = -E_{onset} - 4.93$ (eV).

b) $E_{LUMO} = E_{HOMO} + Eg_{op}$, the optical band gap ($Eg_{op}^{DDF2o}$, the value was 3.0 eV for compound DDF2o in toluene; Eg_{op}^{MDPA}, the value was 3.4 eV for crystal MDPA) was estimated from the onset of the absorption band.

c) Singlet energies E(S$_1$) were calculated from absorption and fluorescence spectra of the compound DDF2o and crystal MDPA, that is, $E(S_1) = 1241/[(\lambda_{abs}+\lambda_{fl})/2]$

d) Triplet energies E(T$_1$) were due to phosphorescence spectra of compound DDF2o and crystal MDPA with the formula $E(T_1) = 1241/\lambda_{ph}$.[17]

Table S2. Characterization of the MDPA crystals and the MDPA:DDF2o crystals. Single-crystal structures were determined by single-crystal X-ray diffraction analysis.

	MDPA	MDPA:DDF2o
Empirical formula	$C_{13}H_{13}N$	$C_{13}H_{13}N$
Crystal system	Orthorhombic	Orthorhombic
Space group	P c c n	P c c n
a(Å)	17.9980(2)	18.0056(5)
b(Å)	15.4512(2)	15.4491(4)
c(Å)	7.50250(10)	7.5013(2)
α(°)	90	90
β(°)	90	90
γ(°)	90	90
Volume(Å^3)	2086.38(5)	2086.64(10)
Z	8	8
Formula weight	183.24	183.24
ρ_{calc}(g/cm^3)	1.167	1.167
λ (Cu Kα) Å	1.54184	1.54184
μ(mm^{-1})	0.518	0.518
2θ range(°)	7.54 - 146.446	7.54 -146.472
Reflections collected	36546	13437
Independent reflections	2076 [R_{int} = 0.0284, R_{sigma} = 0.0080]	2071 [R_{int} = 0.0225, R_{sigma} = 0.0110]
R indexes [I>=2σ (I)]	R 1 = 0.0497, WR 2 = 0.1534	R_1 = 0.0465, wR_2 = 0.1277
R indexes [all data]	R 1 = 0.0540, wR 2 = 0.1590	R_1 = 0.0508, wR_2 = 0.1344
Goodness of fit	1.023	1.040

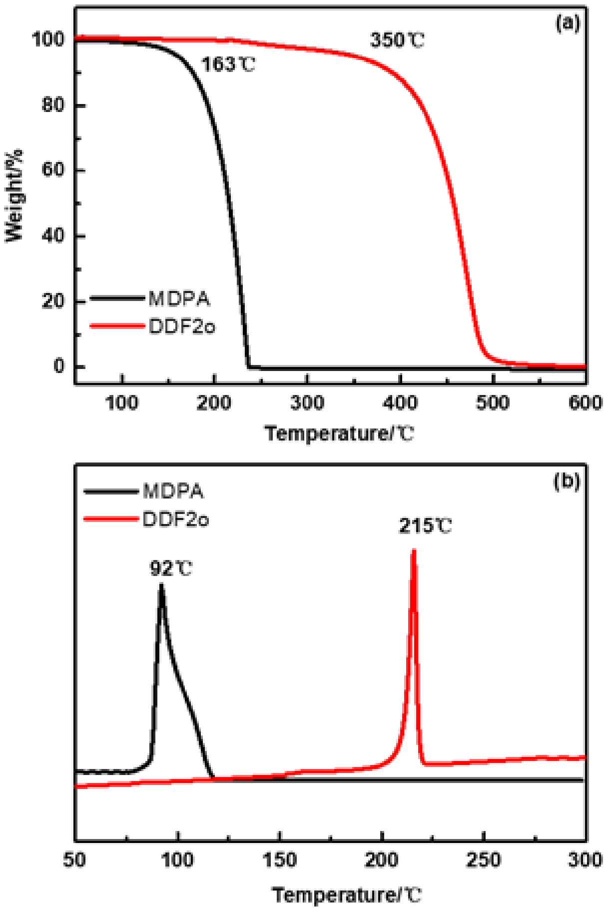

Fig. S1 TGA (a) and DSC (b) curves of MDPA (black) and DDF2o (red).

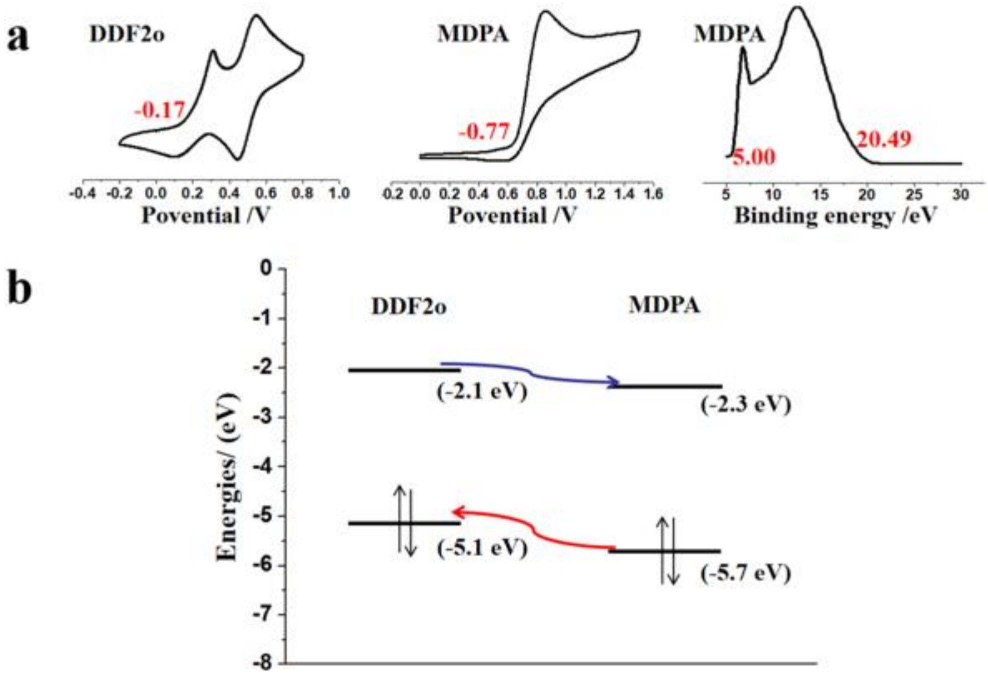

Fig. S2 (a) Electrochemical curves of DDF2o (left) and MDPA (middle) in dichloromethane vs Ag/Ag$^+$, with the concentration of 5×10^{-3} mol•L^{-1}, and UPS spectra with corresponding HOMO of MDPA (right), E_{HOMO} (MDPA_{UPS})=20.49-5.00-21.22=-5.73 (eV). (b) Orbital energy levels of MDPA and DDF2o determined electrochemically, which calculated methods were showed in Table S1. The blue and red lines indicate the possible electron and hole transfers, respectively.

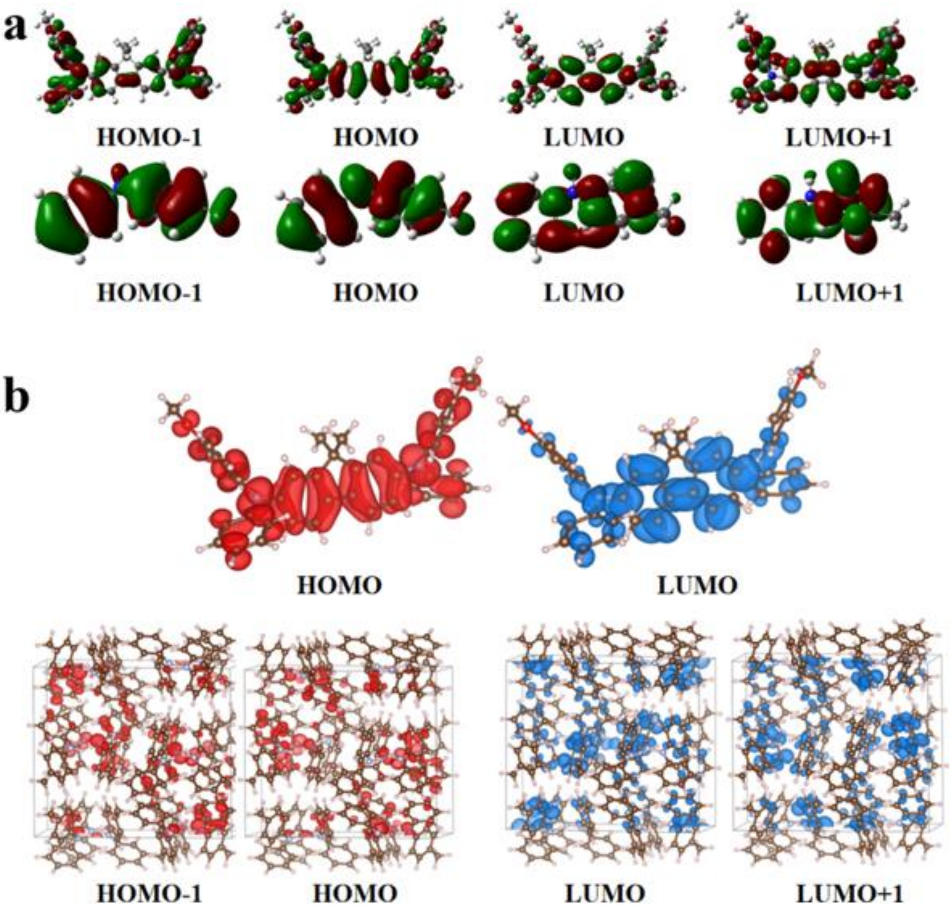

Fig. S3 Frontier molecular orbitals of DDF2o (up) and MDPA (down) using B3LYP/6-311G (d, p) in toluene (a) and those of DDF2o (up) and MDPA crystal (down) from VASP calculations (b).

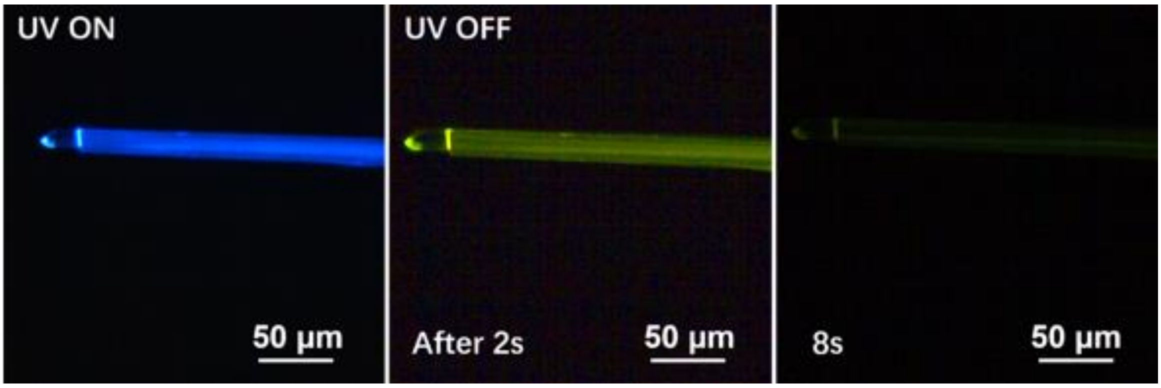

Fig. S4 Photographs of LPL from the MDPA:DDF2o crystals under fluorescence microscope at the 365 nm excitation. (Fabrication of crystals: MDPA accompanied with 1 mol% DDF2o powder were added into dichloromethane under argon atmosphere of glovebox, and the crystals were grown by slow evaporation at room temperature)

,

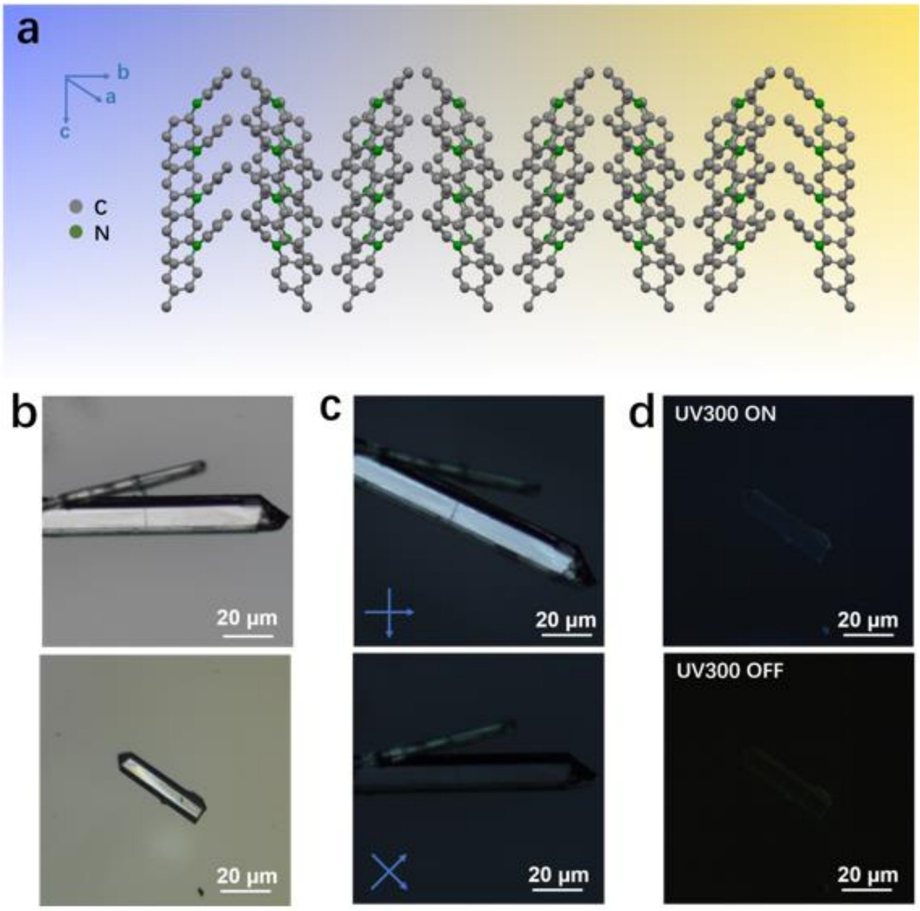

Fig. S5 (a) Partial view of a three-dimensional packing structure of the MDPA crystals, in which hydrogen atoms were omitted for the sake of clarity. (b) Optical microscope images, and (c) polarized microscope images of the MDPA crystals--arrows indicating relative polarizer direction. (d) Photographs of very weak visible photoluminescence of the MDPA crystals at 300 nm excitation at room-temperature and demonstration that LPL emission was not presented after turning off the excitation.

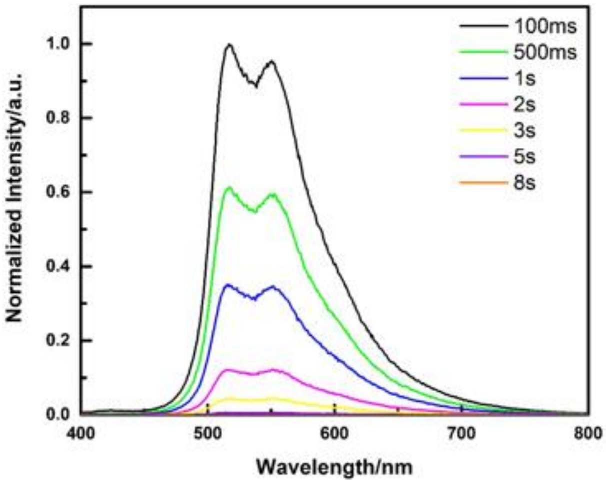

Fig. S6 LPL spectra of the MDPA:DDF2o crystals following excitation with 365 nm (excitation power: 10 mW; excitation time: 2 s; sample temperature: 300 K).

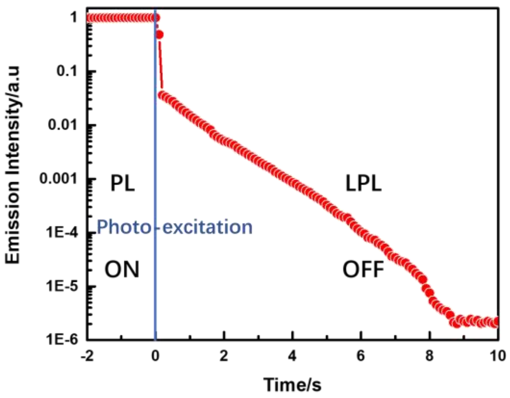

Fig. S7 Semi-logarithmic plot of the emission decay profile of the MDPA:DDF2o crystals prepared in nitrogen atmosphere (excitation wavelength: 365 nm; excitation power: 10 mW; excitation time: 2 s; sample temperature: 300 K).

3. **References**

[1] A. D. Becke, *Phys. Rev. A*, 1988, **38**, 3098-3100.

[2] A. D. Becke, *J. Chem. Phys*., 1993, **98**, 5648-5652.

[3] C. Lee, W. Yang, R. G. Parr, *Phys. Rev. B*, 1988, **37**, 785-789.

[4] J. P. Perdew, K. Burke and M. Ernzerhof, *Phys. Rev. Lett*., 1996, **77**, 3865.

[5] E. Cancès, B. Mennucci and J. Tomasi, *J. Chem. Phys*., 1997, **107**, 3032-3041.

[6] M. J. Frisch, Gaussian 16, Revision C.01,; Gaussian, Inc., Wallingford, CT, USA, 2016.

[7] T. Wang, K. C. Weerasinghe, D. Liu, W. Li, X. Yan, X. Zhou and L. Wang, *J. Mater. Chem. C*, 2014, **2**, 5466-5470.

[8] T. Wang, K. C. Weerasinghe, H. Sun, X. Hu, T. Lu, D. Liu, W. Hu, W. Li, X. Zhou and L. Wang, *J. Phys. Chem. C,* 2016, **120**, 11338-11349.

[9] G. Kresse and J. Hafner, *Phys. Rev. B,* 1993, **48**, 13115.

[10] G. Kresse and J. Furthmüller, *Phys. Rev. B,* 1996, **54**, 11169.

[11] G. Kresse and D. Joubert, *Phys. Rev. B*, 1999, **59**, 1758.

[12] P. E. Blöchl, *Phys. Rev. B*, 1994, **50**, 17953.

[13] L. Wang, J. I. Williams, T. Lin and C.J. Zhong, *Catal. Today*, 2011, **165**, 150-159.

[14] C. Wu, L. Wang, Z. Xiao, G. Li and L. Wang, *Phys. Chem. Chem.Phys*., 2020, **22**, 724-733.

[15] G. M. Sheldrick, SHELXS 97, Program for solution of crystal structure, University of Göttingen: Göttingen, 1997.

[16] G. M. Sheldrick, SHELXL 97, Program for the refinement of crystal structures, University of Göttingen: Göttingen, 1997.

[17] Y. D. Zhang, Y. Wu, Y. Xu, Q. Wang, K. Liu, J. W. Chen, J. J. Cao, C. Zhang, H. Fu and H. L. Zhang, *J. Am. Chem. Soc*., 2016, **138**, 6739-6745.